Article

Interactive Effects Determine Radiocarbon Abundance in Soil Fractions of Global Biomes

Guoai Li [1], Xuxu Chai [1], Zheng Shi [2] and Honghua Ruan [1,*]

[1] Department of Ecology, Co-Innovation Center for Sustainable Forestry in Southern China, Nanjing Forestry University, Nanjing 210037, China
[2] Department of Microbiology and Plant Biology, Institute for Environmental Genomics, University of Oklahoma, Norman, OK 73019, USA
[*] Correspondence: hhruan@njfu.edu.cn

Abstract: Soil organic carbon (SOC) is heterogeneous, consisting of fractions with differing turnover rates. Climate, vegetation, and soil properties can all affect the characteristics of these different soil carbon fractions. However, there has been little investigation into the interactive effects of biotic and abiotic drivers on a large spatial scale. In this study, we utilized data from the international soil radiocarbon database (ISRaD) to investigate the radiocarbon abundance (an indicator of carbon persistence) in soil fractions from several different biomes. Bulk SOC was categorized into three fractions according to the density fractionation method: a free light fraction (fLF), an occluded light fraction (oLF) and a heavy fraction (HF). In addition to the impacts of significant factors such as depth and climate, interactive effects between soil fractions and environmental factors on radiocarbon abundance were prevalent. Specifically, there were significant interactions between climate, vegetation types, soil properties, and soil fractions affecting Δ^{14}C levels. The difference in Δ^{14}C of the shallow depth fractions was significant in the temperate forest, and was not significant in the boreal and tropical forests. The interactive effect between mean annual temperature (MAT) and mean annual precipitation (MAP) on Δ^{14}C was significant in the shallower depth (i.e., 0–30 cm and 30–60 cm) of the oLF and in the deeper soils (i.e., 30–60 cm and 60–100 cm) of the HF. Soil properties also interact with soil fractions in determining Δ^{14}C. After accounting for depth effect, oxalate-extractable aluminum (Alo) accounted for 63.5% of the remaining Δ^{14}C variation in the fLF and accounted for 35.9% of the remaining Δ^{14}C variation in the oLF. Rather than Alo, cation exchange capacity (CEC) accounted for 46.1% of the remaining Δ^{14}C variation in the HF. These findings suggest that the way the interactions between climate, vegetation, and soil properties affect soil carbon persistence at various fractional depths is critical for the accurate prediction of soil carbon dynamics.

Keywords: soil organic carbon (SOC); radiocarbon; Δ^{14}C; soil fractions; soil formation factors; climate change; soil depth

1. Introduction

Soil organic carbon (SOC) is the largest carbon pool in terrestrial ecosystems [1]. As a source and sink of atmospheric CO_2, it plays a critical role in global carbon cycling [2,3]. Changes in SOC can significantly impact the climate system by regulating atmospheric CO_2 concentration. Previous studies have extensively examined soil carbon dynamics in response to climate change. For example, Crowther et al. (2016) predicted a significant loss of soil carbon due to global warming based on data from climate change experiments, but this conclusion was challenged by van Gestel et al. (2018) who added more data points and reported a net neutral change in soil carbon [4]. Global warming can increase vegetation productivity, promoting plant carbon input, but it also enhances microbial activity and accelerates organic matter decomposition. However, it remains controversial whether the increase in vegetation productivity can offset the potential loss of soil carbon [5,6].

In addition, the sensitivity of soil organic carbon to temperature change is a combination of the sensitivity of the various carbon pools [7]. According to Arrhenius theory, the rate of decomposition is inversely proportional to the activation energy of organic matter [8,9]. The active carbon pool has low activation energy, and therefore it has a fast turnover rate [10]. In contrast, the inert carbon pool contains a higher proportion of substances with high activation energy, resulting in slower turnover rates [5,9]. According to the Arrhenius formula, higher activation energy corresponds to greater temperature sensitivity, implying that inert carbon pools have higher temperature sensitivity than active carbon pools. However, the studies by Chen et al. (2021) and Heckman et al. (2022) show that the protective effect of minerals hinders the sensitivity of organic matter to temperature, and the easy-to-decompose carbon pool has higher temperature sensitivity, whereas temperature has a limited effect on the recalcitrant carbon pool [11,12]. Consequently, comprehending the impact of temperature change on soil carbon pools is essential to resolving this debate.

Previous studies have often assumed soil to be a homogeneous and stable bulk. However, bulk soil is not homogeneous, but rather a mixture of multiple pools with different functions. The main determinants affecting soil carbon persistence vary across pools [13]. Therefore, in order to fully understand soil carbon dynamics, it is necessary to investigate the nature of several pool functions. Soil carbon fractionation generally aims to separate fractions according to differences in soil organic matter protection mechanisms [14]. For example, the density fractionation method categorizes the bulk soil organic carbon as three common fractions: a free light fraction (fLF), an occluded light fraction (oLF) and a heavy fraction (HF).

Each of the three carbon fractions has different preservation mechanics, and therefore a different decomposition rate. The fLF is composed of mineral-free particulate organic matter with a high average decomposition rate. It usually contains fresh or mildly decayed plant debris and charcoal [15,16]. The fLF contains repositories of unstable carbon that are important to the terrestrial ecosystem. The oLF has a greater amount of decomposed organic matter than the fLF [17]. It is mainly composed of humified organic matter, charred particulate organic matter, fungal spores and pollen [17–19]. The oLF is thought to turnover at intermediate rates, possibly due to the preservation of complex biomolecules, which are resistant and tightly bound to soil minerals [20]. For example, studies have shown that charcoal is easily encapsulated by mineral particles [21,22]. In addition to charcoal, the oLF also contains a high proportion of Alkyl C and aromatic C, which are resistant to chemical oxidation and have a long duration [23]. The HF is composed of organic matter strongly combined with clay minerals and microbes [15,16]. This fraction mainly consists of nitrogen-containing substances and polysaccharides such as proteins and nucleic acids [18].

Radiocarbon (^{14}C) measurement is a common method used to study soil carbon turnover [23]. Radiocarbon is a radioactive isotope, and its measurement can facilitate the evaluation of the turnover rates of long-term stable carbon pools on different timescales based on natural decay rates [24]. As early nuclear weapons tests injected a large amount of ^{14}C into the atmosphere, the tests were subsequently suspended in order to limit radioactive fallout [23]. The ^{14}C produced by the nuclear explosions was assimilated into the carbon reservoir. Due to the influence of various biological, physical and chemical processes, ^{14}C levels vary in carbon pools with different turnover rates. Soil radiocarbon measurement has been widely used to characterize the stability and turnover rate of SOC. In general, the higher the ^{14}C, the faster the turnover rate of the soil carbon pool.

The persistence of carbon in soil is determined by several factors [18,25,26]. Previous research indicates that the molecular structure of organic matter has a secondary role in regulating carbon persistence, while organisms and the environment play a more significant role [5,23]. A study by Chen et al. (2021) showed that the primary factors regulating soil Δ^{14}C are related to depth. Carbon persistence in surface soil can be affected by various factors and mechanisms, with plant carbon input and climatic factors being the main reasons for the instability of soil organic matter. On the one hand, the input of vegetation

litter and roots include simulating the activity of microorganisms, thus accelerating the turnover of SOC. On the other hand, newly grown plant roots secrete organic acids such as oxalic acid, which break down mineral-protected aggregates, thus accelerating the decomposition of old carbon [11]. The above mechanisms have a limited impact on deep soil. The carbon persistence of deep soil is mainly regulated by mineral protection, and the mineral–organic combination reduces the decomposition rate of soil organic matter [27].

An exceptional study by Heckman and Hicks Pries et al. (2022) has revealed the Δ^{14}C levels in the different carbon fractions and their regulators. Heckman and Hicks Pries et al. (2022) reported a higher amount of Δ^{14}C in the fLF than in the oLF and the HF, and the Δ^{14}C in all the three fractions decreased with soil depth. What remains to be investigated is the difference in soil radiocarbon among the three fractions by depth, and how the differences vary according to differences in climate, biomes and soil properties. In order to achieve this goal, we categorized the soil depth as three discrete layers and investigated the interactive effects of climate, biomes, and soil type on radiocarbon in each of the three layers. Building upon the study of Heckman et al. and Hicks Pries (2022), we further explored the interaction between depth, climate, vegetation, and soil properties in influencing radiocarbon abundance. In our study, the following questions are explicitly addressed: (1) how vegetation, soil depth (three discrete layers) and fractions interact with each other to determine ^{14}C abundance; (2) how temperature and precipitation interact and affect ^{14}C abundance in each fraction along the depths; and (3) how soil properties interact with vegetation and soil fraction in affecting ^{14}C abundance.

2. Methods

A dataset from the International Soil Radiocarbon Database (ISRaD has been developed as a collaboration between the U.S. Geological Survey Powell Center and the Max Planck Institute for Biogeochemistry; www.soilradiocarbon.org (accessed on 16 April 2021) [28] was used to assess the relationship between the persistence of SOC (i.e., Δ^{14}C) and climate, according to the factors of mean annual temperature (MAT) (n = 425) and mean annual precipitation (MAP) (n = 425), soil depths (n = 1300), vegetation types (n = 672) and soil properties (oxalate-extractable Al (Alo), oxalate-extractable Fe (Feo), and cation exchange capacity (CEC)) in the fLF (n = 109), oLF (n = 68) and HF (n = 114).

2.1. Data Source and Processing

The ISRaD is an online repository of environmental radiocarbon data, covering a wide range of spatial scales, with an emphasis on soil radiocarbon, soil fractions and various environmental factors. The dataset used in this study consisted of 1300 Δ^{14}C data points from 295 soil profiles in 113 sampling sites, covering eight major vegetation types from around the world.

To explore the relative importance of different factors in regulating the prevalence of SOC, the effects of climate, vegetation and soil properties were analyzed. The variables included soil radiocarbon abundance (Δ^{14}C), soil density fractions, MAT, MAP, soil depths, vegetation types, and physicochemical properties (Alo, Feo and CEC).

2.1.1. Soil Radiocarbon

1. Soil radiocarbon Δ^{14}C

The radiocarbon data in the ISRaD were compared with accepted standard values for known ^{14}C content ($\left[0.95 \frac{^{14}C}{^{12}C}\right]_{OX1,-19}$). Radiocarbon content was reported as Fraction Modern (Fm) [29].

$$\text{Fraction Modern (FM)} = \left[\frac{\left[\frac{^{14}C}{^{12}C}\right]_{sample,-25}}{\left[0.95\frac{^{14}C}{^{12}C}\right]_{OX1,-19}}\right] \qquad (1)$$

The numerator is the ratio of ^{14}C to ^{12}C, reflecting the rate of decomposition and radioactive decay of a given organic matter pool, corrected for mass-dependent isotope fractionation to Δ^{13}C value of $-25‰$. The denominator is an absolute equal to 95% of the oxalic acid activity measured in 1950 [23].

$$\Delta^{14}C = \left[F_m \times e^{(1950-y)/8267} - 1 \right] \times 1000 \qquad (2)$$

Equation (2) is used to convert Fm into Δ^{14}C (unit in ‰). The variable y represents the measurement year. $e^{(1950-y)/8267}$ is used to correct for the standard decay since 1950 [30].

2. The depth of the soil profile was the middle point between the top and the bottom of the measured depth interval, and was divided into three layers: a shallow layer (0–30 cm), a middle layer (30–60 cm) and a deep layer (60–100 cm).

3. The radiocarbon data were reported in three density fractions of soil carbon: a free light fraction (fLF), an occluded light fraction (oLF) and a heavy fraction (HF). The density fractionation was dependent on the density agent sodium polytungstate. The fLF (<1.65 g cm^{-3}) was the fraction floated in a dense liquid, composed of mineral-free particulate organic matter. The oLF (1.60–2.0 g cm^{-3}) was composed of particulate organic matter released after 5 min of vigorous mixing and ultrasonic disruption. After the removal of these two particulate fractions, the residual organic matter was the HF (>2.0 g cm^{-3}) composed of microbial products that strongly bind to soil minerals [1].

2.1.2. Climate

The climate data consisted of MAT and MAP and were obtained from the World Climate Database (http://www.worldclim.org (accessed on 16 April 2021)) according to the geographic coordinates of each sampling site. The MAT varied from -15 °C to 30 °C and the MAP ranged between 0 and 4000 mm yr^{-1}.

2.1.3. Vegetation Types

The sources of vegetation type factors were studies obtained from the MODIS land cover database. In order to remain consistent with the reported observations, by combining some vegetation types, we reduced the sixteen vegetation types from MODIS into eight. All 1126 forests were reclassified based on latitude as boreal (>50° N), temperate (>23° and <50° N and S) or tropical forests (<23° N and S). Cultivated winter wheat/soybean types were combined as cropland, and the rest remained unchanged. The other vegetation types were grassland, shrubland, savannas and tundra.

2.1.4. Soil Properties

The physical and chemical properties and weathering of rocks can strongly affect soil properties. Several previous studies have shown that the persistence of C in soil is associated with soil properties such as mineral types and surface charges. Three forms of Fe and Al oxides, as well as cation contents, are indicators of the probability of substantial amounts of SOC protected by minerals. These are oxalate-extractable Fe/Al oxides (Feo + Alo), pyrophosphate-extractable Fe/Al oxides (Fep + Alp) and dithionite-extractable Fe/Al oxides (Fed + Ald). Feo + Alo were mainly selected for analysis in this study (n_{Feo} = 385, n_{Alo} = 385). Feo + Alo represent poorly crystalline oxy-hydroxides and organically complexed Fe/Al oxides, which have a large surface area and high surface activity, promoting the formation and stability of large agglomerates through cementation [31]. CEC (n_{CEC} = 237) reflects the ability of the soil to adsorb positive charges at the negative charge positions on the surface of soil minerals and organic matter, and to form loose electrostatic bonds. It can affect the stability of soil structure and nutrient availability, affecting the level of soil fertilizer retention [32]. It is an important soil property affecting the prevalence of SOC.

2.2. Statistical Analyses

2.2.1. Δ^{14}C in Different Depth Intervals, Density Fractions, and Biomes

First, an analysis of variance (ANOVA) [33] was used to assess differences in soil radiocarbon abundance Δ^{14}C in varying depth and density fractions (sample size n = 1300). When the ANOVA test was significant (i.e., $p < 0.05$), we used multiple comparison (Tukey test) [34] to determine the difference between any given pair of depth or density fractions. Next, we followed the same procedure to compare Δ^{14}C among differing soil fractions and among three forest ecosystems (boreal, temperate, and tropical) in shallow depth (0–30 cm) (n = 672). Only data from forest ecosystems in shallow depth were selected for the analysis, due to the low sample size in other biomes and forest ecosystems of high depth.

2.2.2. Relationships of Δ^{14}C with Depth and Climate

We used a linear mixed-effect model (LMM) [35] to explore how soil density fractions interact with depth and climate factors (MAT and MAP) and influence soil radiocarbon abundance (n = 1246). In the LMM, the soil profile was used as random factor. When there were significant interactions between MAT and MAP in determining Δ^{14}C, we divided MAP into two parts: MAP $\leq$ 1000 mm yr^{-1} (drier condition) and MAP > 1000 mm yr^{-1} (wetter condition). We then performed the LMMs analysis separately and fitted it according to the results. Note that we did not include soil properties in this analysis, due to the much smaller sample size of soil properties in the datasets. Rather, the primary aim was to explore the effects of interactions among depth, fractions and climates on radiocarbon abundance. Soil properties are included in the analysis below.

2.2.3. Relationships of Δ^{14}C with Soil Properties

The role of soil properties in affecting radiocarbon abundance was then further explored, using a small subset of the database (n = 291), in the following section. First, forward elimination was applied to select significant variables among depth, climate, and soil properties [36]. The threshold was chosen as 0.05, so only variables below that threshold were selected. The potential predictors included depth, MAT, MAP, Alo, Feo and CEC.

Then, LMM was used to examine the relationships between predictors and radiocarbon abundance, with biomes as the random factor. To illustrate the relationships, we fitted a simple linear model to demonstrate the relationship between radiocarbon and the first selected variable, depth. The selected predictors were then progressively added to the LMMs, to fit the residuals of the response variable Δ^{14}C after controlling for the depth effect with the subsequent predictor variables.

3. Results

A total of 113 sampling sites were used in our study, covering eight major biomes (Figure 1a). Most of the sampling sites (67 out of 113) were in the US and western Europe. Forty-four sampling sites were temperate forest and nineteen were grassland. There were only four sites in the tundra and six in boreal forest. The sampling sites spanned a wide range of climatic conditions, with a MAT of −14–27 °C, and a MAP of 0–3800 mm (Figure 1b). The temperate forest sites were distributed within a narrower range of climatic conditions, with a MAT of 5–15 °C and a MAP of 0–2000 mm. Most of the tropical sites were warm (MAT > 20 °C) and humid (MAP > 2000 mm). The two tropical sites with the lowest MAT were in coastal regions. The four tundra sites were the coldest and the driest. The boreal sites were warmer and more humid than the tundra sites. The two cool grassland sites with the lowest MAT were at high elevation.
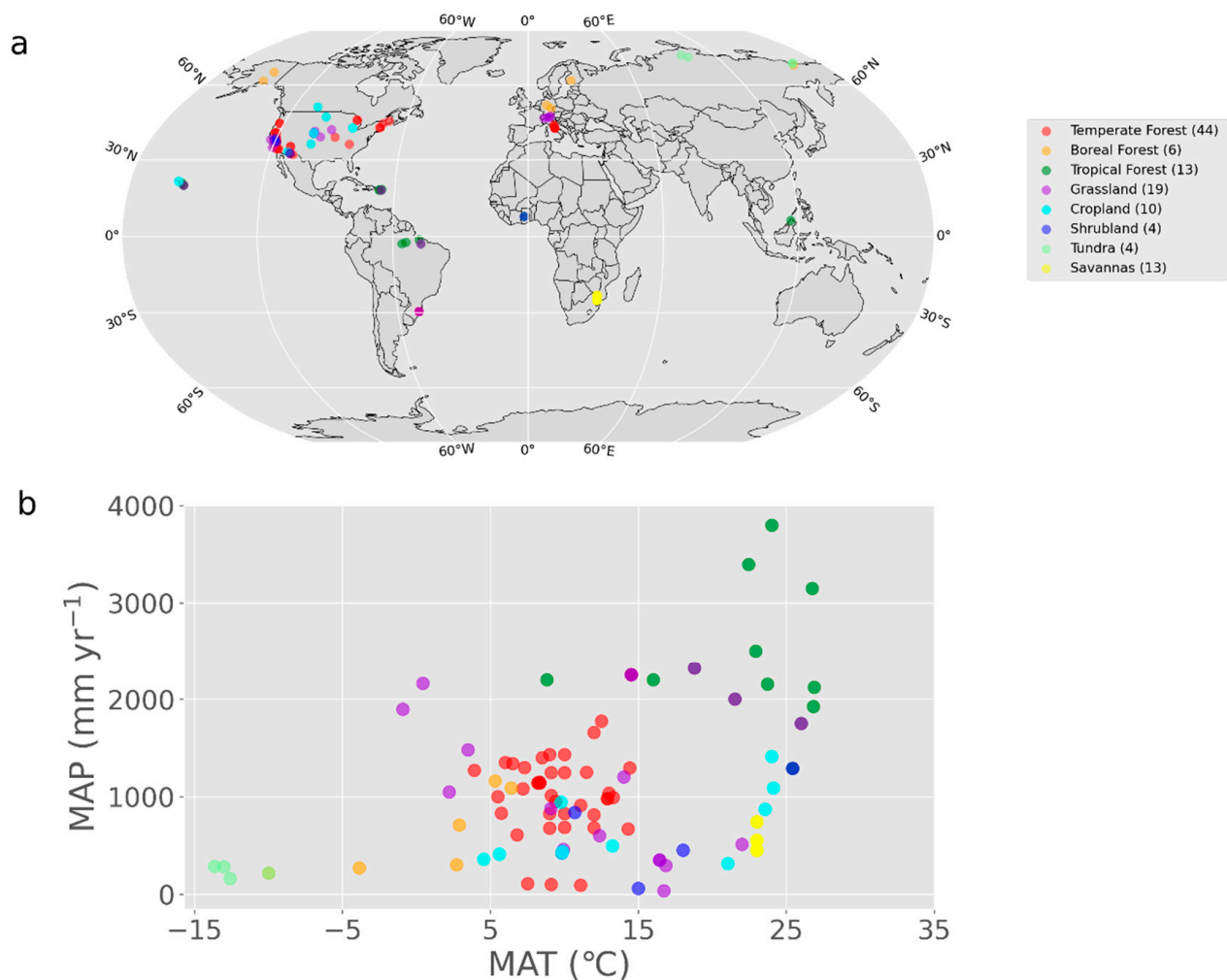
Figure 1. Global distribution and climatic conditions of the soil sampling sites. (**a**) The map shows the geographic location of the soil sampling sites. Vegetation types are color-coded. The eight vegetation types are temperate forest (n = 44), boreal forest (n = 6), tropical forest (n = 13), grassland (n = 19), cropland (n = 10), shrubland (n = 4), tundra (n = 4), and savanna (n = 13). The numbers in the brackets are sampling sites. In a few cases, there are two vegetation types in one sampling site. (**b**) The radiocarbon measurement points cover the major vegetation types and climatic zones. MAT and MAP varied greatly.

The Δ^{14}C decreased with depth in the three fractions (Figure 2). Δ^{14}C decreased faster in the oLF (95%CI of the slope: $[-6.91, -5.54]$) and the HF (95%CI of the slope: $[-5.14, -4.50]$) than in the fLF (95%CI of the slope: $[-3.67, -2.70]$). There were significant interactions between depths and fractions in determining Δ^{14}C. At the shallow depth (0–30 cm), Δ^{14}C was the largest in the fLF (mean: $49.14 \pm 4.69‰$) and the lowest in the HF (mean: $-3.05 \pm 4.64‰$). The oLF contained $17.81 \pm 6.49‰$ Δ^{14}C at the shallow depth. However, in the deeper soils (30–60 cm and 60–100 cm), Δ^{14}C was the highest in the fLF ($-104.79 \pm 21.04‰$ at 30–60 cm and $-168.44 \pm 39.68‰$ at 60–100 cm), but there was no difference between the oLF ($-196.62 \pm 28.58‰$ at 30–60 cm and $-429.14 \pm 67.53‰$ at 60–100 cm) and the HF ($-168.03 \pm 14.91‰$ at 30–60 cm and $-358.26 \pm 29.06‰$ at 60–100 cm).
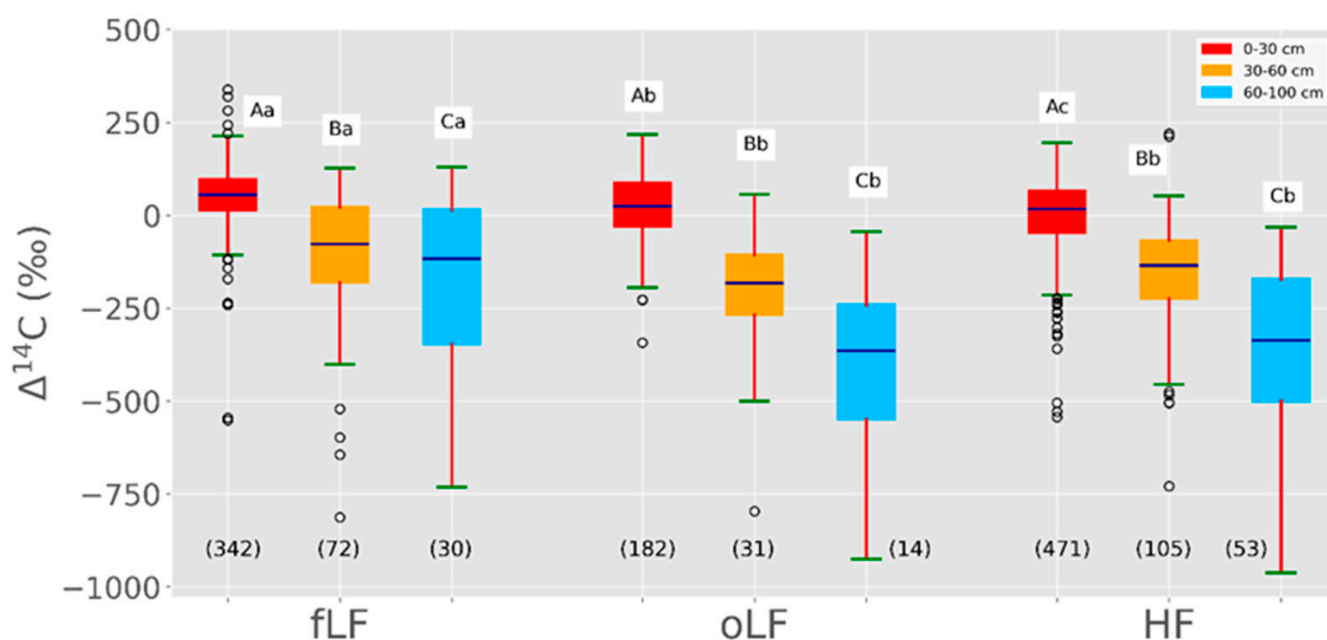
Figure 2. Depth distribution of $\Delta^{14}C$ in different carbon fractions. Blue lines indicate the median values, boxes indicate 1st and 3rd quartiles, whiskers represent 5 and 95% confidence intervals, open dots are outliers and n represents the sample size for each group. Different letters indicate significant differences ($p < 0.05$) between groups. Capital letters indicate the differences between the different depths of the same fraction. Lowercase letters indicate the differences between different fractions of the same depth.

There were significant interactions between vegetation types and fractions in determining $\Delta^{14}C$ values at the shallow depth (Figure 3). The difference in $\Delta^{14}C$ between fractions was only significant in the temperate forest, not significant in the boreal and tropical forests. In the temperate forest, the $\Delta^{14}C$ level was higher in the fLF (mean: 58.67 ± 4.66‰) and lower in the oLF (mean: 23.26 ± 6.25‰) and the HF (mean: 17.65 ± 4.63‰), but showed no difference between the oLF and the HF. $\Delta^{14}C$ in the boreal forests was -28.12 ± 26.43‰ in the fLF, -67.48 ± 17.26‰ in the oLF and -76.78 ± 22.18‰ in the HF, and $\Delta^{14}C$ in the tropical forest was 28.62 ± 35.47‰ in the fLF, 26.84 ± 37.67‰ in the oLF and 24.36 ± 14.68‰ in the HF. In all fractions, $\Delta^{14}C$ in the temperate and tropical forest ecosystems was consistently greater than in the boreal forest. However, there was no difference in $\Delta^{14}C$ between temperate and tropical forest.

In addition to soil depth, climatic conditions (i.e., MAT and MAP) also influenced the variation in $\Delta^{14}C$ between the three fractions. The three factors were all important for interpreting $\Delta^{14}C$ while considering the whole soil depth down to one meter (and Table 1). Together, the three factors accounted for 65.1%, 75.9% and 61.9% of the $\Delta^{14}C$ variation in the fLF, oLF and HF. Soil $\Delta^{14}C$ strongly increased with MAT in the three fractions (Table 1), and $\Delta^{14}C$ increased faster in the oLF (95%CI: [6.76, 17.31]) than that in the fLF (95%CI: [7.15, 12.06]) and the HF (95%CI: [5.05, 10.91]). Although MAP showed no significant relationship with $\Delta^{14}C$ in the fLF and oLF, there were significant interactions between MAT and MAP in determining $\Delta^{14}C$ in the HF.
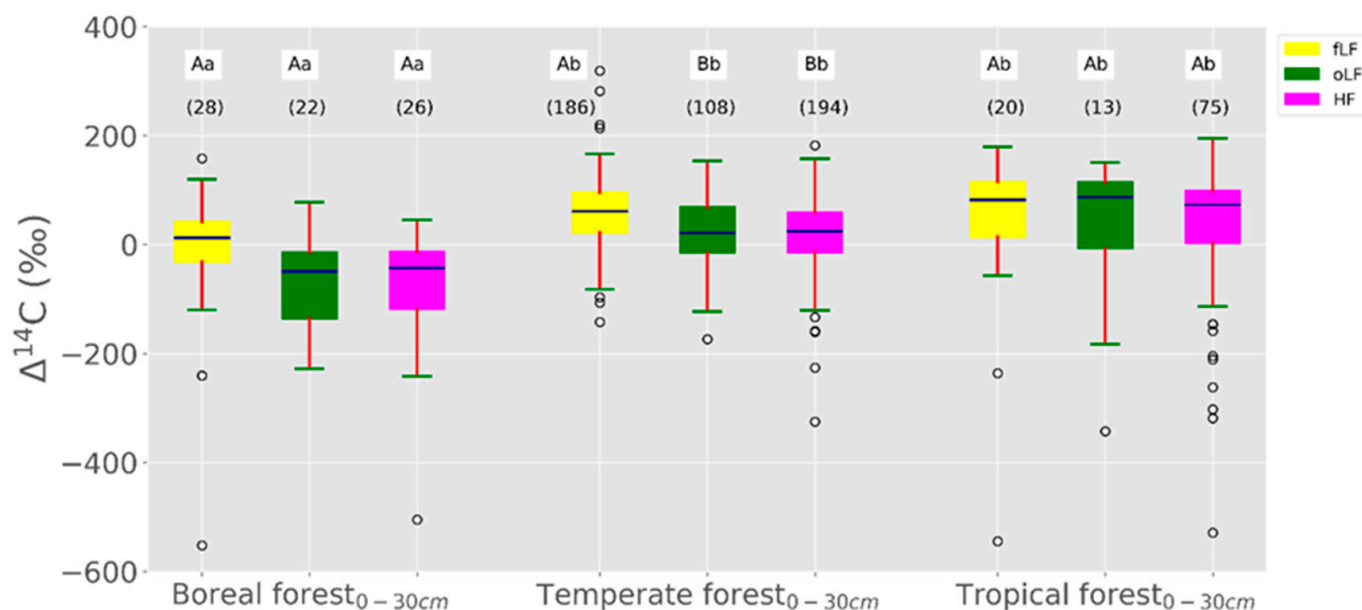
Figure 3. Comparison of soil $\Delta^{14}C$ in the three fractions at 0–30 cm under the three vegetation types. The vegetation types were boreal forest, temperate forest, and tropical forest. Blue lines indicate the median values, boxes indicate the 1st and 3rd quartiles, whiskers represent 5% and 95% confidence intervals, open dots are outliers and n represents the sample size for each group. Different letters indicate significant differences in $\Delta^{14}C$ between groups ($p < 0.05$), and capital letters indicate differences between different fractions of the same vegetation type. Lowercase letters indicate differences between different vegetation types of the same fraction. We did not conduct the same analyses in other biomes and depths due to low sample size.

Table 1. Results of liner mixed-effect model regression for effects of the fractions, depths, and climates (MAT and MAP) on soil radiocarbon abundance ($\Delta^{14}C$). MAT is mean annual temperature. MAP is mean annual precipitation.

Fraction Property	Intercept	Coef	*p*
Free light	Depth	−2.77	0.00
	MAT	9.60	0.00
	MAP	0.04	0.06
	MAT × MAP	0.00	0.00
Occluded light	Depth	−5.00	0.00
	MAT	12.04	0.00
	MAP	0.04	0.26
	MAT × MAP	−0.01	0.02
Heavy fraction	Depth	−1.46	0.00
	MAT	8.00	0.00
	MAP	0.07	0.00
	MAT × MAP	0.00	0.00

　　　Next, a mixed-effect linear model was used to investigate the climatic regulating effects on $\Delta^{14}C$ in the three fractions at three different depths (Table 2). Depth became a less important factor for the oLF $\Delta^{14}C$ in deep soil (60–100 cm). MAT was a significant factor accounting for the variation of $\Delta^{14}C$ in the fLF and oLF in the shallower depth (0–30 cm and 30–60 cm), but not in greater depth (60–100 cm). However, MAT was a significant factor accounting for the variation of $\Delta^{14}C$ in the HF at all depths. The interactive effect between MAT and MAP was significant in the shallower depth (i.e., 0–30 cm and 30–60 cm) for explaining $\Delta^{14}C$ in the oLF, but was always more significant in the deeper soils (i.e., 30–60 cm and 60–100 cm) in the HF (Figure 4). Generally, we found that $\Delta^{14}C$ increased

with MAT under drier conditions but decreased with MAT under more humid conditions (Figure 4).

Table 2. Results of linear mixed-effect model regression showing the effects of depths and climates on the Δ^{14}C level in three fractions at different depths.

Fraction Property	Depth (cm)	Intercept	Coef	*p*
Free light	0–30	Depth	−5.00	0.00
		MAT	4.93	0.02
		MAP	−0.01	0.55
		MAT × MAP	0.00	0.28
	30–60	Depth	−4.08	0.03
		MAT	14.95	0.00
		MAP	0.13	0.10
		MAT × MAP	−0.01	0.06
	60–100	Depth	0.18	0.92
		MAT	5.94	0.54
		MAP	0.11	0.70
		MAT × MAP	−0.01	0.77
Occluded light	0–30	Depth	−6.81	0.00
		MAT	10.80	0.00
		MAP	0.02	0.49
		MAT × MAP	0.00	0.02
	30–60	Depth	−6.03	0.04
		MAT	22.38	0.02
		MAP	0.19	0.18
		MAT × MAP	−0.03	0.02
	60–100	Depth	−7.09	0.00
		MAT	57.47	0.22
		MAP	1.71	0.17
		MAT × MAP	−0.14	0.18
Heavy fraction	0–30	Depth	−5.88	0.00
		MAT	5.25	0.00
		MAP	0.02	0.30
		MAT × MAP	0.00	0.24
	30–60	Depth	−4.19	0.01
		MAT	7.86	0.00
		MAP	0.04	0.38
		MAT × MAP	−0.01	0.01
	60–100	Depth	−2.60	0.10
		MAT	16.29	0.00
		MAP	0.23	0.01
		MAT × MAP	−0.02	0.00

Lastly, LMM was used to investigate the relationships between soil properties and Δ^{14}C in the three fractions, with a much smaller sample size than the above analyses due to a low availability of data on properties (Figures 5–7). A stepwise regression was used to reveal that climate was not a significant factor in the analyses. As expected, soil depth was consistently the dominant factor for interpreting the variation in Δ^{14}C. Soil properties. rather than climate conditions, were the secondary factors accounting for the remaining variation in Δ^{14}C. After depth, Alo accounted for 63.5% of the rest of the Δ^{14}C variation in the fLF (Figure 5) and 35.9% of the remaining Δ^{14}C variation in the oLF (Figure 6), and CEC accounted for 46.1% of the remaining Δ^{14}C variation in the HF (Figure 7).
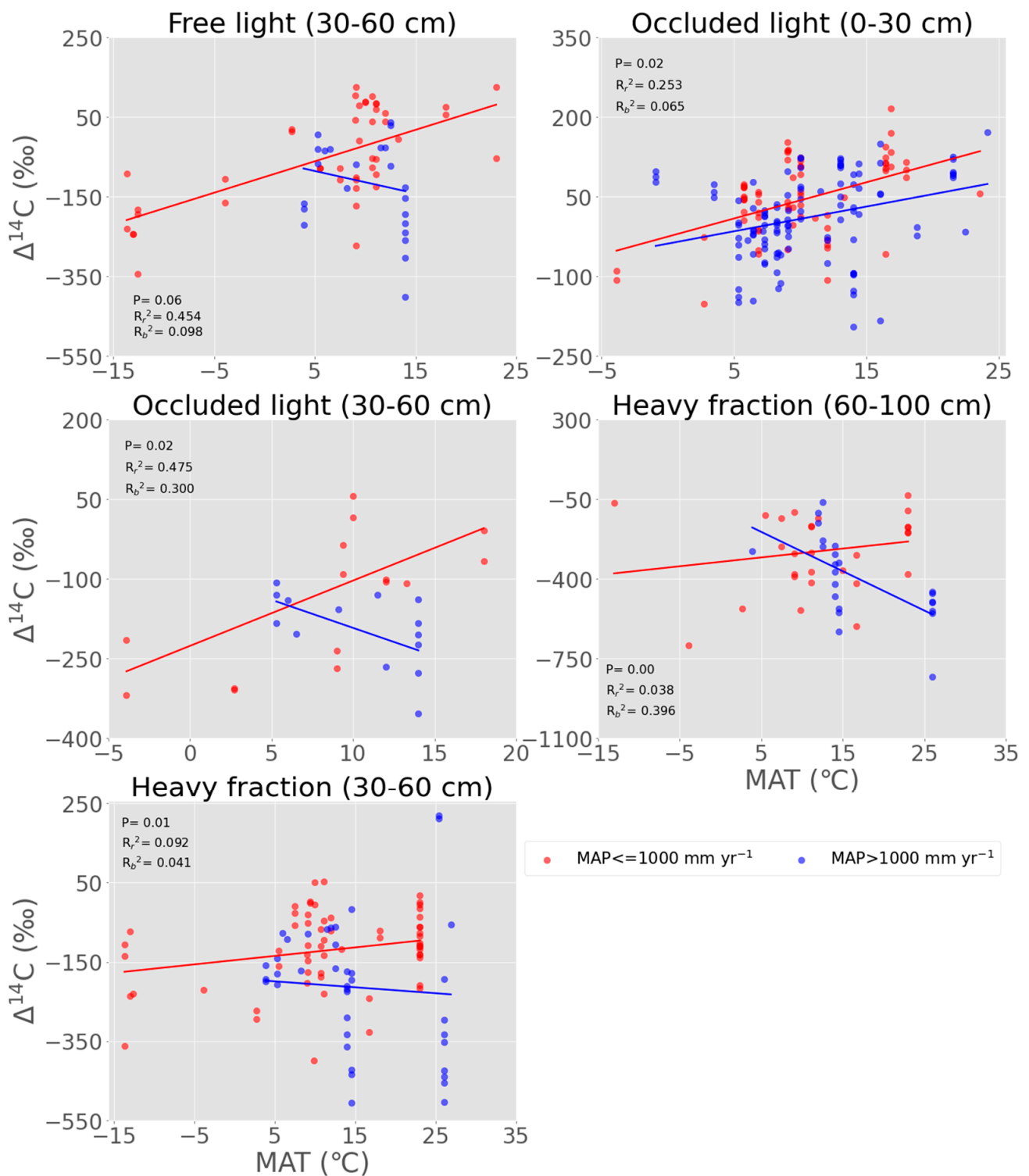
Figure 4. Relationships between soil radiocarbon abundance (Δ^{14}C) and MAT in different fractions and depths. Data were divided by fractions (fLF, oLF, HF) and depths (0–30 cm, 30–60 cm, 60–100 cm). The red and blue solid lines indicate an interaction between MAT and MAP and correspond to the regression fitting line at MAP $\leq$ 1000 mm yr^{-1} and MAP > 1000 mm yr^{-1}.

Figure 5. Relationships between soil radiocarbon abundance (Δ^{14}C) and soil depth/mineral protections, including Feo, Alo and cation exchange capacity (CEC) in the free light fraction.

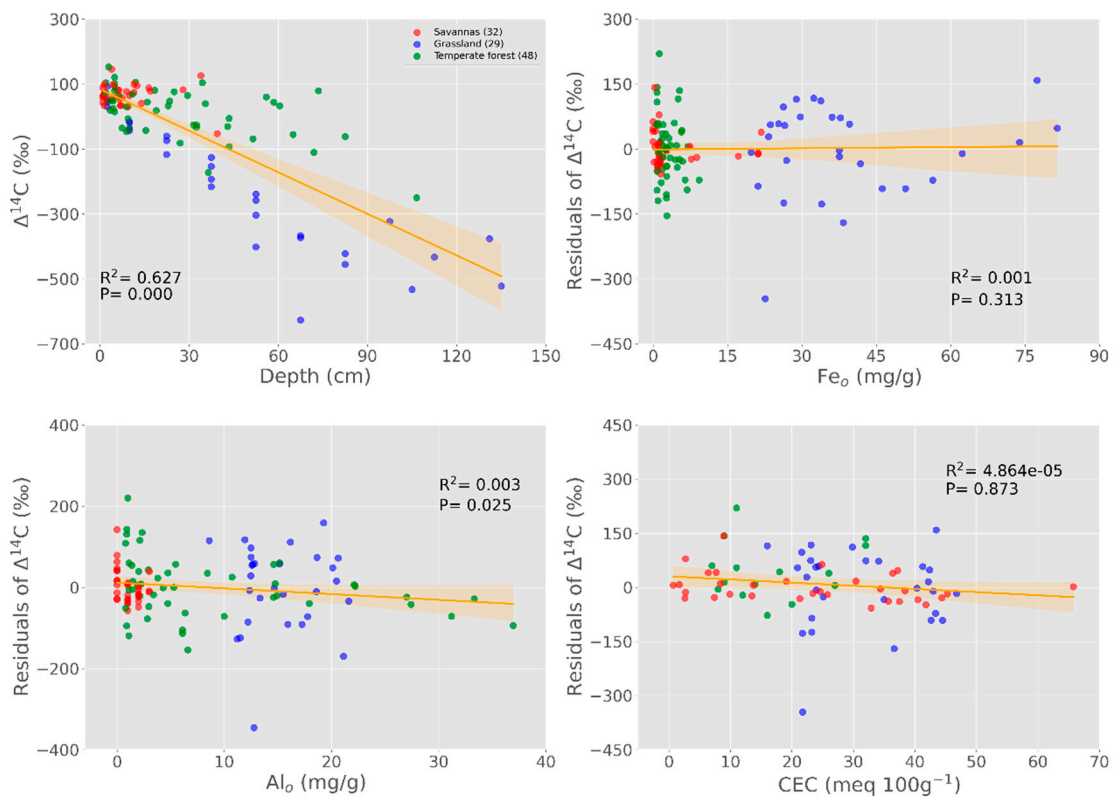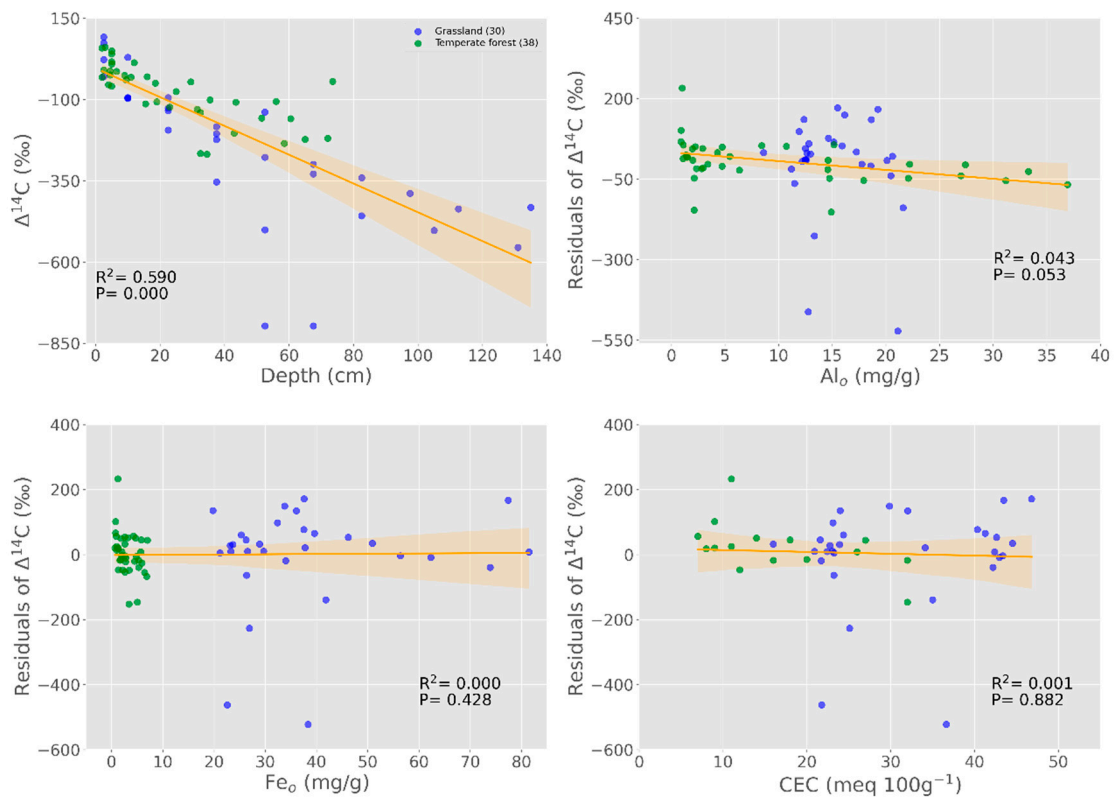**Figure 6.** Relationships between soil radiocarbon abundance (Δ^{14}C) and soil depth/mineral protections, including Feo, Alo and cation exchange capacity (CEC) in the occluded light fraction (oLF).
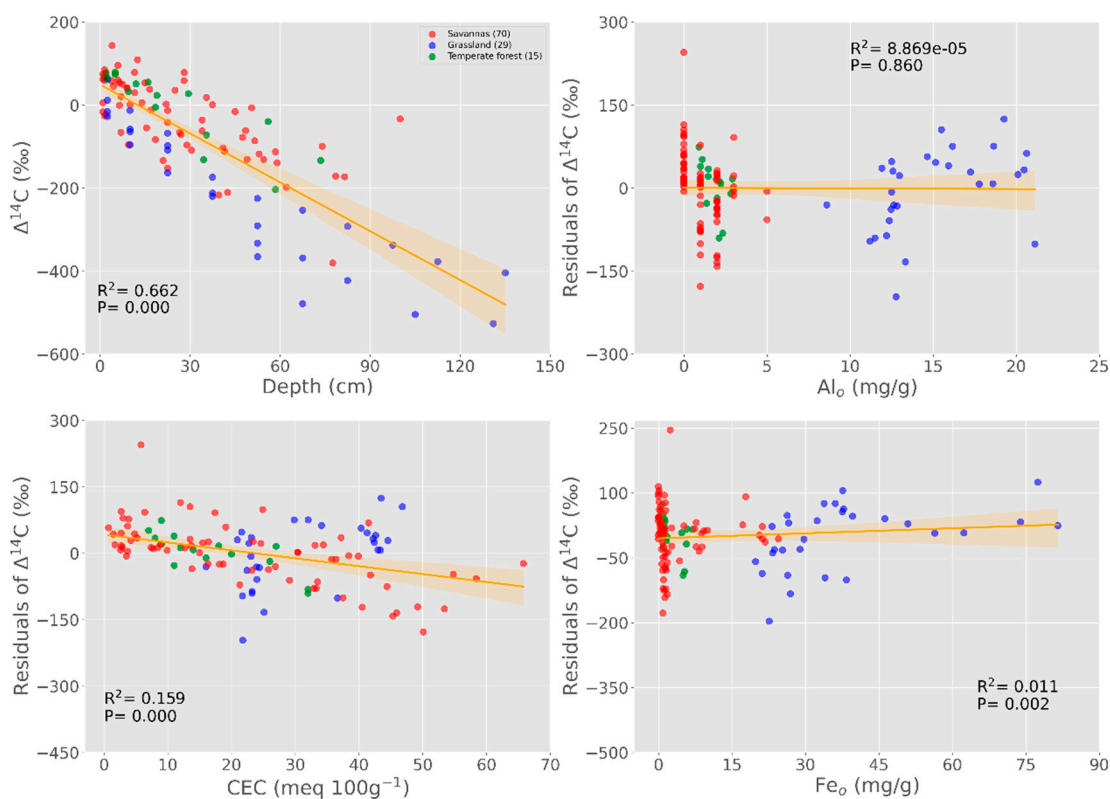
Figure 7. Relationships between soil radiocarbon abundance (Δ^{14}C) and soil depth/mineral protections, including Feo, Alo and cation exchange capacity (CEC) in the heavy fraction (HF).

4. Discussion

In addition to a depth-dependent decrease in Δ^{14}C, we found that soil carbon fractions were related with both depths and vegetation types in determining Δ^{14}C in this study. We also found significant interactions between the two climatic factors, MAT and MAP, in regulating Δ^{14}C in different soil carbon fractions. Lastly, we showed that soil properties outweighed climate as factors accounting for the spatial variation of Δ^{14}C in all soil carbon fractions, using a smaller dataset. Moreover, our analyses suggest that the depth-dependent decrease in bulk soil Δ^{14}C [30] was at least partly caused by the Δ^{14}C in each of the soil carbon fractions.

4.1. Interactive Effect of Depth and Soil Carbon Fractions

Depth and soil fractions are important determinants of soil carbon abundance and persistence [12,30]. In this study, we observed significant interactions between depths and fractions in determining Δ^{14}C. Δ^{14}C decreased faster in the oLF and the HF than that in the fLF. In soil profiles, the topsoil is an open system with constant fresh litter inputs. The fLF has rapid turnover rates due to a lack of mineral protection. This explains why the oLF and the HF show sharp decreases in soil Δ^{14}C level, with increases of soil depth compared to the fLF. Furthermore, the input of fresh organic matter decreases with soil depth, which most strongly affects the fLF [37]. Secondly, as the soil depth increases, the microbial biomass and the sensitivity of carbon decomposition to temperature gradually decrease [38], impeding the decomposition processes. This process probably affects the fLF the most. Thirdly, aggregation and mineral content increase with depth, which provides strong protection to the oLF and the HF, but not to the fLF [39].

Previous studies have shown that soil radiocarbon abundance decreases with depth, and different soil fractions have different levels of radiocarbon content [40]. However, none of the studies have specifically assessed what determines the depth-dependency. Is it caused by a higher proportion of aggregate and mineral protected carbon at greater depth,

or because the radiocarbon content also decreases with depth in each soil fraction? Our results show that radiocarbon depleted with depth in each of the soil fractions, but to a greater degree in the oLF and the HF. The difference in the Δ^{14}C values of the soil density fraction suggests that the protective mechanism determines the turnover time. Globally, the fLF consists of mineral-free particulate organic matters with low to average decomposition rates [15,16]. This fraction has the highest Δ^{14}C value and the fastest turnover rate, and climate variables and vegetation types play key roles. The oLF consists of organic matter, microbes, and mineral particles [25,41]. A lower Δ^{14}C value of this fraction indicates a longer duration of the organic carbon. This may be due to mineral protection, as the reduced accessibility of microorganisms and their extracellular enzymes leads to organic matter retention [42]. The continuous existence of complex and/or condensed aromatic biomolecules such as charcoal in the oLF makes the fraction of organic carbon more stable [43,44]. The organic carbon in the HF is derived from microorganisms and adsorbed on clay minerals to form a mineral–organic complex [45]. Chemical forces such as hydrogen bonds, intermolecular force and ionic bonds prevent organic carbon decomposition [18], causing the turnover of this fraction to be slow and the Δ^{14}C value to be low. Therefore, the oLF and the HF may be more heavily influenced by soil mineral properties.

4.2. Interactive Effect of Vegetation Types and Fractions

In this study, it was observed that the Δ^{14}C value varied among different soil fractions in temperate forests, with the fLF having the highest value and the oLF and HF having the lowest values. with no difference shown between the oLF and the HF. It has been found that in topsoil (0–30 cm), plant carbon input plays a dominant role in Δ^{14}C variation. The fLF is mainly composed of mineral particle-free organic matter, which has a faster turnover rate than the other two fractions, resulting in a higher Δ^{14}C value. Additionally, it was found that the Δ^{14}C value was consistently greater in temperate and tropical forests than in boreal forests, which may be due to the low plant carbon input in boreal forest ecosystems and the cold and dry climate that favors the long-term preservation of soil organic matter. These findings suggest that climatic variables play a critical role in determining the soil carbon persistence in the topsoil.

4.3. Interactive Effect of MAT and MAP

Globally, climate change determines carbon abundance by affecting its input and output [46]. This is because climate affects vegetation productivity, driving root growth and litter production. Temperature and moisture can also influence the catabolic effect of microorganisms on organic carbon, thus affecting carbon distribution and turnover [23]. In addition, climate factors are also closely related to soil mineral characteristics. Climate factors can indirectly influence organic carbon dynamics by interacting with soil factors. All of these interactions can lead to dramatic changes in the soil radiocarbon content [47]. In conclusion, climate factors and their interactions can have strong effects on the distribution, turnover, and stability of soil organic carbon [48].

4.3.1. Temperature

Temperature is widely considered to be an important influence on soil carbon persistence. Previous studies have viewed the soil as a whole, noting that short-term temperature increases promote an exponential increase in microbial enzymatic activity, thus directly accelerating organic carbon decomposition and mineralization [49]. However, there have been few studies on how carbon pools respond to temperature changes. We found that soil Δ^{14}C strongly increased with MAT in all three fractions. However, when the temperature increased, Δ^{14}C increased faster in the oLF than that in the fLF and the HF. This may be because the increase in temperature causes increased microbial activity inside the aggregate structure, activating some of the protective mechanisms in the oLF, and the organic carbon decomposes more easily. When consumed by decomposers, it transforms into a microbial product and merges into the HF. It also may be the case that recalcitrant substrates have

a higher sensitivity to temperature, with increased temperatures facilitating the decomposition of organic matter. Therefore, decomposition in the oLF accelerates faster with increasing temperature than in the fLF [5].

Additionally, the temperature sensitivity of the carbon pools is different at each depth layer. When studying the temperature sensitivity of each fraction at differing depth layers, we found that the regulating effect of MAT on soil $\Delta^{14}C$ is associated with depth. Increased MAT reduced $\Delta^{14}C$ in all fractions, but in the topsoil the effect of MAT on $\Delta^{14}C$ was most significant. In contrast, organic carbon in the subsoil is less sensitive to warming, so MAT has less impact on changes in subsoil $\Delta^{14}C$. Therefore, in the context of global warming, the temperature increase may not strongly affect carbon reserves and their persistence in the subsoil.

4.3.2. Moisture

MAP is an important driver of radiocarbon content. Similar to the effects of MAT, the effects of MAP on $\Delta^{14}C$ also varied by depth. Firstly, rainfall can contribute to increased vegetation productivity, which explains why the topsoil $\Delta^{14}C$ values increased with increasing MAP. MAP is even more important for soil carbon persistence in subsoil than in topsoil [12]. This is because rainfall can transfer young, fresh soluble organic carbon to deep soil. Rainfall can also help increase the depth of plants' roots, thus maintaining root carbon in the subsoil [48]. All of these factors can facilitate the formation of new carbon pools in the subsoil. Our findings show that in addition to these effects, a moderate increase in humidity under warm conditions also increases microbial activity and promotes organic carbon decomposition [3]. This is because water can increase the diffusion of microbial enzymes and improve the availability of soil organic matter. This could explain why $\Delta^{14}C$ increases with increasing MAP in the case of MAP $\leq$ 1000 mm yr^{-1}, when moisture is a limiting factor.

However, greater water availability causes microbial hypoxia, which reduces the rate of microbial decomposition [5]. Secondly, higher water levels will drive soil weathering and increase surface area adsorption, and polyvalent cations can dissolve from the upper soil, accelerating the combination of minerals and organic carbon in the deep soil [50,51]. Furthermore, higher moisture levels result in reduced iron and aluminum, as they cause them to be oxidized and form a chelating complex of organic carbon with iron or aluminum ions [52]. These chelating complexes are water-soluble and can move down in the topsoil in the water and precipitate out into the deep soil. All these factors can improve the persistence of SOC. This explains why $\Delta^{14}C$ decreases with increasing MAP in the case of MAP > 1000 mm yr^{-1}.

4.4. Interactive Effect of Soil Properties

In addition to vegetation and climatic factors, mineral properties are also important factors affecting soil carbon persistence [53]. We know that once the organic matter enters the soil, it undergoes microbial decomposition and reaches a stable state by combining with the soil mineral particles to form aggregates [54–56]. SOC can be physically protected by becoming encapsulated in soil aggregates, and it can also be combined with minerals, thereby increasing the energy required for microbial decomposition and reducing its decomposition rate [51,54]. Our data show that the $\Delta^{14}C$ values decreased with increasing aluminum oxide content in both the fLF and the oLF. This may be because iron and aluminum oxides are tightly bound to organic compounds through covalent bonds, forming organic–mineral complexes, and reducing soil carbon effectiveness, which promotes their conservation in the soil [57,58]. In addition, the $\Delta^{14}C$ value decreased with increasing polyvalent cation content in the HF. This may be because a polyvalent cation bridge is formed on the negatively charged mineral surface by the adsorption of polyvalent cations in the HF, which is critical to explaining the stability of SOC in the HF [18,59]. The strong adsorption effect can stabilize the soil organic matter, preventing microbial degradation and leaching [26,60]. However, it remains unknown why different soil properties determine

radiocarbon abundance in different soil fractions. In summary, soil mineral properties contribute to soil carbon persistence, significantly associated with the Δ^{14}C values of each fraction.

5. Conclusions

The determinants of soil carbon persistence vary among different soil density fractions, and are not influenced by a single factor but co-regulated in different ways. In soil profiles, soil depth was the primary factor driving Δ^{14}C changes in all carbon pools, and soil carbon persistence increased with depth. However, Δ^{14}C in the oLF and the HF decreased faster than in the fLF. This may be due to the effects associated with increased depth, including the reduced accessibility of microorganisms and their extracellular enzymes to organic matter with depth. Soil aggregates and mineral content increased with depth, providing strong "protection" for organic matter in the oLF and the HF. In forest ecosystems, we found that Δ^{14}C levels varied among different soil fractions, and the Δ^{14}C level in the fLF was significantly greater than in the oLF and the HF. Moreover, climate variables are significant determinants of soil carbon persistence. Specifically, MAT had a greater impact on Δ^{14}C change in topsoil than in the subsoil. There were significant interactions between MAT and MAP in determining Δ^{14}C. Our findings suggest that the interactive effects of several factors are important in determining soil carbon persistence.

Author Contributions: Conceptualization, H.R. and Z.S.; methodology, G.L. and X.C.; validation, G.L., X.C. and Z.S.; formal analysis, G.L.; data curation, G.L.; writing—original draft preparation, G.L.; writing—review and editing, H.R. and Z.S.; funding acquisition, H.R. All authors have read and agreed to the published version of the manuscript.

Data Availability Statement: The data that support the findings of this study are available online: www.soilradiocarbon.org (accessed on 16 April 2021).

Conflicts of Interest: The authors declare no conflict of interest.

References

1. Wagai, R.; Mayer, L.M.; Kitayama, K. Nature of the 'occluded' low-density fraction in soil organic matter studies: A critical review. *Soil Sci. Plant Nutr.* **2009**, *55*, 13–25. [CrossRef]
2. Jackson, R.B.; Lajtha, K.; Crow, S.E.; Hugelius, G.; Kramer, M.G.; Piñeiro, G. The Ecology of Soil Carbon: Pools, Vulnerabilities, and Biotic and Abiotic Controls. *Annu. Rev. Ecol. Evol. Syst.* **2017**, *48*, 419–445. [CrossRef]
3. Lal, R. Soil carbon sequestration impacts on global climate change and food security: Soils: The final frontier. *Science (Am. Assoc. Adv. Sci.)* **2004**, *304*, 1623–1627. [CrossRef]
4. Van Gestel, N.; Shi, Z.; Van Groenigen, K.J.; Osenberg, C.W.; Andresen, L.C.; Dukes, J.S.; Hovenden, M.J.; Luo, Y.; Michelsen, A.; Pendall, E.J.N. Predicting soil carbon loss with warming. *Nature* **2018**, *554*, E4–E5. [CrossRef] [PubMed]
5. Davidson, E.A.; Janssens, I.A. Temperature sensitivity of soil carbon decomposition and feedbacks to climate change. *Nature* **2006**, *440*, 165–173. [CrossRef] [PubMed]
6. Kirschbaum, M.U. The temperature dependence of soil organic matter decomposition, and the effect of global warming on soil organic C storage. *Soil Biol. Biochem.* **1995**, *27*, 753–760. [CrossRef]
7. Belay-Tedla, A.; Zhou, X.; Su, B.; Wan, S.; Luo, Y. Labile, recalcitrant, and microbial carbon and nitrogen pools of a tallgrass prairie soil in the US Great Plains subjected to experimental warming and clipping. *Soil Biol. Biochem.* **2009**, *41*, 110–116. [CrossRef]
8. Kleber, M.; Nico, P.S.; Plante, A.; Filley, T.; Kramer, M.; Swanston, C.; Sollins, P. Old and stable soil organic matter is not necessarily chemically recalcitrant: Implications for modeling concepts and temperature sensitivity. *Glob. Chang. Biol.* **2011**, *17*, 1097–1107. [CrossRef]
9. Knorr, W.; Prentice, I.; House, J.; Holland, E.J.N. Long-term sensitivity of soil carbon turnover to warming. *Nature* **2005**, *433*, 298–301. [CrossRef]
10. John, B.; Yamashita, T.; Ludwig, B.; Flessa, H. Storage of organic carbon in aggregate and density fractions of silty soils under different types of land use. *Geoderma* **2005**, *128*, 63–79. [CrossRef]

11. Chen, L.; Yang, Y.; Cleland, E. Response to Comment on 'Soil carbon persistence governed by plant input and mineral protection at regional and global scales'. *Ecol. Lett.* **2021**, *24*, 2529–2532. [CrossRef]
12. Heckman, K.; Hicks Pries, C.E.; Lawrence, C.R.; Rasmussen, C.; Crow, S.E.; Hoyt, A.M.; Fromm, S.F.; Shi, Z.; Stoner, S.; McGrath, C.; et al. Beyond bulk: Density fractions explain heterogeneity in global soil carbon abundance and persistence. *Glob. Chang. Biol.* **2022**, *28*, 1178–1196. [CrossRef] [PubMed]
13. Trumbore, S.E. Potential responses of soil organic carbon to global environmental change. *Proc. Natl. Acad. Sci. USA* **1997**, *94*, 8284–8291. [CrossRef]
14. von Luetzow, M.; Koegel-Knabner, I.; Ekschmitt, K.; Flessa, H.; Guggenberger, G.; Matzner, E.; Marschner, B. SOM fractionation methods: Relevance to functional pools and to stabilization mechanisms. *Soil Biol. Biochem.* **2007**, *39*, 2183–2207. [CrossRef]
15. Sollins, P.; Spycher, G.; Topik, C. Processes of Soil Organic-Matter Accretion at a Mudfloe Chronosequence, Mt. Shasta, California. *Ecology* **1983**, *64*, 1273–1282. [CrossRef]
16. Spycher, G.; Sollins, P.; Rose, S. Carbon and nitrogen in the light fraction of a forest soil: Vertical distribution and seasonal patterns. *Soil Sci.* **1983**, *135*, 79–87. [CrossRef]
17. Golchin, A.; Oades, J.M.; Skjemstad, J.O.; Clarke, P. Study of Free and Occluded Particulate Organic-Matter in Soils by Solid-State C-13 Cp/Mas Nmr-Spectroscopy and Scanning Electron-Microscopy. *Aust. J. Soil Res.* **1994**, *32*, 285–309. [CrossRef]
18. Baisden, W.T.; Amundson, R.; Cook, A.C.; Brenner, D.L. Turnover and storage of C and N in five density fractions from California annual grassland surface soils. *Glob. Biogeochem. Cycles* **2002**, *16*, 61–64. [CrossRef]
19. Wagai, R.; Mayer, L.M.; Kitayama, K.; Knicker, H. Climate and parent material controls on organic matter storage in surface soils: A three-pool, density-separation approach. *Geoderma* **2008**, *147*, 23–33. [CrossRef]
20. Brodowski, S.; John, B.; Flessa, H.; Amelung, W. Aggregate-occluded black carbon in soil. *Eur. J. Soil Sci.* **2006**, *57*, 539–546. [CrossRef]
21. Aber, J.D.; Melillo, J.M.; McClaugherty, C.A. Predicting long-term patterns of mass loss, nitrogen dynamics, and soil organic matter formation from initial fine litter chemistry in temperate forest ecosystems. *Can. J. Bot.* **1990**, *68*, 2201–2208. [CrossRef]
22. Conant, R.T.; Ryan, M.G.; Ågren, G.I.; Birge, H.E.; Davidson, E.A.; Eliasson, P.E.; Evans, S.E.; Frey, S.D.; Giardina, C.P.; Hopkins, F.M. Temperature and soil organic matter decomposition rates–synthesis of current knowledge and a way forward. *Glob. Chang. Biol.* **2011**, *17*, 3392–3404. [CrossRef]
23. Trumbore, S. Radiocarbon and Soil Carbon Dynamics. *Annu. Rev. Earth Planet Sci.* **2009**, *37*, 47–66. [CrossRef]
24. Trumbore, S.E. Age of soil organic matter and soil respiration: Radiocarbon constraints on belowground C dynamics. *Ecol. Appl.* **2000**, *10*, 399–411. [CrossRef]
25. Golchin, A.; Baldock, J.A.; Clarke, P.; Higashi, T.; Oades, J.M. The effects of vegetation and burning on the chemical composition of soil organic matter of a volcanic ash soil as shown by C-13 NMR spectroscopy 2. Density fractions. *Geoderma* **1997**, *76*, 175–192. [CrossRef]
26. Hemingway, J.D.; Rothman, D.H.; Grant, K.E.; Rosengard, S.Z.; Eglinton, T.I.; Derry, L.A.; Galy, V. Mineral protection regulates long-term global preservation of natural organic carbon. *Nature* **2019**, *570*, 228–231. [CrossRef]
27. Eusterhues, K.; Rumpel, C.; Kleber, M.; Kögel-Knabner, I. Stabilisation of soil organic matter by interactions with minerals as revealed by mineral dissolution and oxidative degradation. *Org. Geochem.* **2003**, *34*, 1591–1600. [CrossRef]
28. Lawrence, C.R.; Beem-Miller, J.; Hoyt, A.M.; Monroe, G.; Sierra, C.A.; Stoner, S.; Heckman, K.; Blankinship, J.C.; Crow, S.E.; McNicol, G. An open-source database for the synthesis of soil radiocarbon data: International Soil Radiocarbon Database (ISRaD) version 1.0. *Earth Syst. Sci. Data* **2020**, *12*, 61–76. [CrossRef]
29. Stuiver, M.; Polach, H.A. Reporting of C-14 Data—Discussion. *Radiocarbon* **1977**, *19*, 355–363. [CrossRef]
30. Shi, Z.; Allison, S.D.; He, Y.; Levine, P.A.; Hoyt, A.M.; Beem-Miller, J.; Zhu, Q.; Wieder, W.R.; Trumbore, S.; Randerson, J. The age distribution of global soil carbon inferred from radiocarbon measurements. *Nat. Geosci.* **2020**, *13*, 555–559. [CrossRef]
31. Li, Z.-Y.; Xu, R.-K.; Li, J.-Y.; Hong, Z.-N. Effect of clay colloids on the zeta potential of Fe/Al oxide-coated quartz: A streaming potential study. *J. Soils Sediments* **2016**, *16*, 2676–2686. [CrossRef]
32. Warner, S.A. Cation Exchange Properties of Forest Litter as Influenced by Vegetation Type and Decomposition. Master's Thesis, Oregon State University, Corvallis, OR, USA, 1976.
33. Ahmad, J. Motion Detection of Camouflaged Targets Using "ANOVA" Technique. Ph.D. Dissertation, University of Florida, Gainesville, FL, USA, 1982.
34. Abdi, H.; Williams, L. Newman-Keuls test and Tukey test. *Encycl. Res. Des.* **2010**, *2*, 897–902.
35. Li, B. *Robust Prediction from Linear Mixed-Effects Models with Applications to Small Area Estimation*; University of California: Davis, CA, USA, 2001.
36. Efroymson, M.A. Multiple regression analysis. In *Mathematical Methods for Digital Computers*; John Wiley & Sons: Hoboken, NJ, USA, 1960; pp. 191–203.
37. Ellerbrock, R.H.; Kaiser, M. Stability and composition of different soluble soil organic matter fractions–evidence from $\delta^{13}C$ and FTIR signatures. *Geoderma* **2005**, *128*, 28–37. [CrossRef]
38. Bradford, M.A.; Wieder, W.R.; Bonan, G.B.; Fierer, N.; Raymond, P.A.; Crowther, T.W.J. Managing uncertainty in soil carbon feedbacks to climate change. *Nat. Clim. Chang.* **2016**, *6*, 751–758. [CrossRef]

39. Ahrens, B.; Guggenberger, G.; Rethemeyer, J.; John, S.; Marschner, B.; Heinze, S.; Angst, G.; Mueller, C.W.; Kögel-Knabner, I.; Leuschner, C.; et al. Combination of energy limitation and sorption capacity explains 14C depth gradients. *Soil Biol. Biochem.* **2020**, *148*, 107912. [CrossRef]

40. Sierra, C.A.; Hoyt, A.M.; He, Y.; Trumbore, S.E. Soil organic matter persistence as a stochastic process: Age and transit time distributions of carbon in soils. *Glob. Biogeochem. Cycles* **2018**, *32*, 1574–1588. [CrossRef]

41. Waters, A.; Oades, J.J.A. Organic matter in water-stable aggregates. *Adv. Soil Org. Matter Res. Impact Agric. Environ.* **1991**, *90*, 163–174.

42. Six, J.; Bossuyt, H.; Degryze, S.; Denef, K. A history of research on the link between (micro)aggregates, soil biota, and soil organic matter dynamics. *Soil Tillage Res.* **2004**, *79*, 7–31. [CrossRef]

43. Krull, E.S.; Swanston, C.W.; Skjemstad, J.O.; McGowan, J.A. Importance of charcoal in determining the age and chemistry of organic carbon in surface soils. *J. Geophys. Res. Biogeosci.* **2006**, *111*, G4. [CrossRef]

44. Preston, C.M.; Schmidt, M.W. Black (pyrogenic) carbon: A synthesis of current knowledge and uncertainties with special consideration of boreal regions. *Biogeosciences* **2006**, *3*, 397–420. [CrossRef]

45. Villarino, S.H.; Pinto, P.; Jackson, R.B.; Piñeiro, G. Plant rhizodeposition: A key factor for soil organic matter formation in stable fractions. *Sci. Adv.* **2021**, *7*, eabd3176. [CrossRef] [PubMed]

46. Parton, W.; Silver, W.L.; Burke, I.C.; Grassens, L.; Harmon, M.E.; Currie, W.S.; King, J.Y.; Adair, E.C.; Brandt, L.A.; Hart, S.C.; et al. Global-scale similarities in nitrogen release patterns during long-term decomposition. *Science* **2007**, *315*, 361–364. [CrossRef] [PubMed]

47. Schuur, E.A.; Druffel, E.R.; Trumbore, S.E. *Radiocarbon and Climate Change*; Springer: Cham, Switzerland, 2016.

48. Schmidt, M.W.; Torn, M.S.; Abiven, S.; Dittmar, T.; Guggenberger, G.; Janssens, I.A.; Kleber, M.; Kögel-Knabner, I.; Lehmann, J.; Manning, D.A. Persistence of soil organic matter as an ecosystem property. *Nature* **2011**, *478*, 49–56. [CrossRef] [PubMed]

49. Trumbore, S.E.; Zheng, S. Comparison of fractionation methods for soil organic matter 14C analysis. *Radiocarbon* **1996**, *38*, 219–229. [CrossRef]

50. Six, J.; Elliott, E.T.; Paustian, K. Soil macroaggregate turnover and microaggregate formation: A mechanism for C sequestration under no-tillage agriculture. *Soil Biol. Biochem.* **2000**, *32*, 2099–2103. [CrossRef]

51. Six, J.; Conant, R.T.; Paul, E.A.; Paustian, K. Stabilization mechanisms of soil organic matter: Implications for C-saturation of soils. *Plant Soil* **2002**, *241*, 155–176. [CrossRef]

52. Chen, L.; Fang, K.; Wei, B.; Qin, S.; Feng, X.; Hu, T.; Ji, C.; Yang, Y. Soil carbon persistence governed by plant input and mineral protection at regional and global scales. *Ecol. Lett.* **2021**, *24*, 1018–1028. [CrossRef]

53. Torn, M.S.; Trumbore, S.E.; Chadwick, O.A.; Vitousek, P.M.; Hendricks, D.M. Mineral control of soil organic carbon storage and turnover. *Nature* **1997**, *389*, 170–173. [CrossRef]

54. Oades, J.M. Soil organic matter and structural stability: Mechanisms and implications for management. *Plant Soil* **1984**, *76*, 319–337. [CrossRef]

55. Masiello, C.A.; Chadwick, O.A.; Southon, J.; Torn, M.S.; Harden, J.W. Weathering controls on mechanisms of carbon storage in grassland soils. *Glob. Biogeochem. Cycles* **2004**, *18*, 4. [CrossRef]

56. Mikutta, R.; Kleber, M.; Torn, M.S.; Jahn, R. Stabilization of Soil Organic Matter: Association with Minerals or Chemical Recalcitrance? *Biogeochemistry* **2006**, *77*, 25–56. [CrossRef]

57. Lalonde, K.; Mucci, A.; Ouellet, A.; Gélinas, Y. Iron promotes the preservation of organic matter in sediments. *Nature* **2012**, *483*, 198–200. [CrossRef] [PubMed]

58. Finley, B.K.; Dijkstra, P.; Rasmussen, C.; Schwartz, E.; Mau, R.L.; Liu, X.-J.A.; van Gestel, N.; Hungate, B.A. Soil mineral assemblage and substrate quality effects on microbial priming. *Geoderma* **2018**, *322*, 38–47. [CrossRef]

59. Rowley, M.C.; Grand, S.; Verrecchia, É.P. Calcium-mediated stabilisation of soil organic carbon. *Biogeochemistry* **2017**, *137*, 27–49. [CrossRef]

60. Kindler, R.; Siemens, J.; Kaiser, K.; Walmsley, D.C.; Bernhofer, C.; Buchmann, N.; Cellier, P.; Eugster, W.; Gleixner, G.; Grünwald, T. Dissolved carbon leaching from soil is a crucial component of the net ecosystem carbon balance. *Glob. Chang. Biol.* **2011**, *17*, 1167–1185. [CrossRef]